MUTATOR PHENOTYPES CAUSED BY SUBSTITUTION AT A CONSERVED MOTIF A RESIDUE IN EUKARYOTIC DNA POLYMERASE δ*

Ranga N. Venkatesan, Jessica J. Hsu, Nicole A. Lawrence[1], Bradley D. Preston and Lawrence A. Loeb

From the Department of Pathology, University of Washington, Seattle, Washington 98195-7705

Running Title: L612 Substitutions in Yeast Pol δ Induces Mutator Phenotypes

Address correspondence to: Lawrence A. Loeb, Department of Pathology, University of Washington, Seattle, Washington 98195-7705**,** Tel. 206 543-6015; Fax. 206 543-3967; E-Mail: laloeb@u.washington.edu

[1]Present address: Abbott Laboratories, Abbott Park, Illinois 60064

Eukaryotic DNA polymerase δ (Pol δ)[1] replicates chromosomal DNA, and is also involved in DNA repair and genetic recombination. Motif A in Pol δ, containing the sequence DxxxLYPSI, includes a catalytically essential aspartic acid as well as other conserved residues of unknown function. Here, we used site-directed mutagenesis to create all 19 amino acid substitutions for the conserved Leu612 in Motif A of *Saccharomyces cerevisiae* Pol δ. We show that substitutions at Leu612 differentially affect viability, sensitivity to genotoxic agents, cell cycle progression and replication fidelity. The eight viable mutants contained Ile, Val, Thr, Met, Phe, Lys, Asn or Gly substitutions. Individual substitutions varied greatly in the nature and extent of attendant phenotypic deficiencies, exhibiting mutation rates that ranged from near wild-type to a 37-fold increase. The L612M mutant exhibited a 7-fold elevation of mutation rate but essentially no detectable effects on other phenotypes monitored; the L612T mutant showed a nearly wild-type mutation rate together with marked hypersensitivity to genotoxic agents; and the L612G and L612N strains exhibited relatively high mutation rates and severe deficits overall. We compare our results with those for homologous substitutions in prokaryotic and eukaryotic DNA polymerases, and discuss the implications of our findings for the role of Leu612 in replication fidelity.

DNA-dependent DNA polymerases display a common catalytic mechanism and play a pivotal role in DNA replication, DNA repair and genetic recombination (1). Sixteen different DNA polymerases have been identified in eukaryotic cells, and are classified into four families (family-A, -B, -Y, and -X) based on sequence homology and presumed function (2). The eukaryotic enzymes in family B, comprised of DNA polymerases-α, -δ, -ε, and -ζ, are involved in DNA replication and also function in other DNA synthetic processes (3). One current replication model suggests that the DNA polymerase α-primase holoenzyme complex initiates *de novo* synthesis of primers, which are then extended by DNA polymerases-δ and -ε (abbreviated as Pol δ and Pol ε respectively) (4-7). Pol δ and Pol ε contain multiple conserved motifs; the N-terminus harbors the 3'→5' proofreading exonuclease and polymerase motifs, while the functions of the C-terminus have not been established.

Pols-δ and -ε synthesize DNA with high fidelity and are highly processive upon interaction with proliferating cell nuclear antigen (PCNA) (8-10). Fidelity is achieved by the sequential, coordinated actions of the polymerase and 3'→5' exonuclease proofreading domains. It has been estimated that Pols-δ and -ε incorporate approximately one non-complementary nucleotide per 10^4 to 10^6 nucleotides polymerized, and that their exonuclease domains further enhance accuracy by 2- to 10-fold (5-7,11). Structure-function studies of mutant DNA polymerases have led to identification of critical residues in conserved motifs A and B in the polymerase domain that affect fidelity of family A, family B and family Y DNA polymerases (12-21). Results from several laboratories demonstrate that

evolutionarily conserved amino acids in motifs A and B that form the nucleotide-binding pocket can tolerate substitutions (12-21). Substitution at motif A and B residues in both prokaryotic and eukaryotic DNA polymerases imparts a wide range of phenotypes, including reduced activity, compromised fidelity, altered substrate specificity, and DNA replication defects (13,20,22-24). However, replacement of any one of a catalytic triad of acidic amino acids, one in motif A and two in motif C**,** results in inactivation (25,26)**.**

In this work, we exploited the evolutionary homology in the catalytic domains of family A and family B DNA polymerases to create mutants of *S.cerevisiae* Pol δ that increase mutation rates. We and others have previously shown that mutation at a conserved Ile in motif A of *E.coli* DNA polymerase I and *Taq* DNA polymerase I alters fidelity (12,15,20,21). Here, we created all 19 replacements for the homologous residue in yeast Pol δ, and found that replacements at this position affect fidelity. We demonstrate that amino acid substitutions at Leu612 in *S. cerevisiae* motif A differentially affect viability, mutation rates, cell cycle progression and sensitivity to genotoxic agents**.**

Experimental Procedures

Yeast strains: Standard recombinant DNA and yeast molecular genetic techniques, including growth media, were followed (27,28). YGL27-3D (*MAT*a *leu2 his3 ade2 trp1 lys2 ura3 pol3::KanMX* or *pol3::HIS3*), a kind gift of Gerard Faye (Institute Curie-Biologie), was the starting point for construction of strains used in this study (29). YGL27-3D harbors a lethal partial deletion of the chromosomal *POL3* gene; *POL3* function is provided by a wild-type copy of the gene carried on the plasmid pGL310, derived from the *URA3* plasmid Ycp50-SUP11 (29). The entire chromosomal copy of *POL3* in YGL27-3D was replaced with a KanMX cassette to yield YGL27-*pol3*Δ (Singh, M. and Preston, B.D., unpublished data). Similarly, we replaced the entire chromosomal copy of *POL3* in the strain BY4741 (*MAT*a *his3-1 leu2Δ met15Δ ura3Δ*) (ATCC, Manassas, VA) with a KanMX cassette to yield BY4741-*pol3*Δ; *POL3* function is provided by a wild-type copy of the gene carried on the plasmid YCplac33 (ATCC, Manassas, VA), which contains *URA3* selectable marker to obtain plasmid Ycplac33-POL3.

Generation of Pol δ mutant strains: To generate amino acid replacements at Leu612 of Pol δ, the plasmid YCplac111-*POL3* was utilized for site-directed mutagenesis using a Quik Change kit (Stratagene, San Diego, CA). YCplac111-*POL3* contains the wild-type *POL3* gene (including its native promoter) cloned into the *LEU2* plasmid YCplac111 (ATCC, Manassas, VA). Nineteen oligonucleotides and their complementary sequences, each pair encoding a different amino acid at position 612, were used in PCR reactions with YCplac111-*POL3* to generate the desired mutations. All the primer sequences are readily available upon request. The presence of the predicted mutation at codon 612, and the absence of additional mutations, was established by sequencing the entire *pol*3 gene, which was then excised from the vector by digestion with *Hind*III/*Eco*RI and cloned into new stock of YCplac111 vector digested with same enzymes. The resulting haploid mutant strains were used for this work. Plasmid shuffling, modeled after the procedure of Simon et al. (29),was used to create Pol δ mutant strains. Plasmids harboring point mutations at Leu612 were transformed individually into YGL27-*pol3*Δ cells by using an EZ-transformation II kit (Zymo Research, Orange, CA). Transformed cells were grown on SC-Leu-Ura plates (28) for 2-3 days to select for both the YCplac111-*pol3*, (*pol3* mutants, Leu marker) and pGL310 (*POL3*, wild-type, Ura marker) plasmids. Controls included transformations with YCPlac 111 (vector alone), wild-type *POL3* and the exonuclease-deficient *pol3-01* allele (D321A, E323A) in YCplac111 (29). The pGL310-*POL3* plasmid was shuffled out by streaking 10-20 colonies on SC-Leu (28) plates containing 5-fluoroorotic acid (5-FOA, ZymoResearch, Orange, CA; 1 mg/ml). Colonies that grew were re-streaked on fresh SC-Leu+5-FOA plates. After 2-3 days, *LEU2* plasmids were rescued from three independent colonies of each "shuffled-out strain" and sequenced to verify the predicted mutations. The same procedures were used to construct *pol3* mutant derivatives in a BY4741 strain background; the haploid BY4741-*pol3* strains were used for FACS analysis, owing to its facile

synchronization with α mating factor and the inability of YGL27-3D strains to respond to α mating factor.

Quantitation of POL3 mRNA expression: Two-step real time RT-PCR was used to quantitate *Pol3* mRNA expression. Overnight cultures of each of the strain were diluted to OD_{600nm}~0.2-0.22, cultured at 30°C and harvested at OD_{600nm} ~0.7-0.72. Total RNA was isolated using hot phenol procedure and 2ug of RNA was digested with RQ1 Dnase (Promega, Madison, WI) to hydrolyze contaminating genomic DNA. cDNA synthesis and PCR reactions were performed using SuperScript III Platinum Two-step qRT-PCR kit with SYBR Green (Invitrogen, Carlsbad, CA) according to manufacturer's instructions. Real-time PCR were performed on DNA Engine Opticon2 instrument and analyzed with supplied software (BioRad, Hercules, CA). The *Pol3* mRNA expression levels were quantitated and normalized to constitutively generated *Ura3* transcript. Standard curves for both *Pol3* and *Ura3* expression were generated by plotting threshold of signal detection against the log of RNA dilution. The amount of RNA used in each reaction was in the linear range as observed from the *Pol3* and *Ura3* standard curves. The threshold values C(t) obtained from amplification profiles were first normalized to internal standard *Ura3* and next to wild-type *Pol3* expression level. The entire procedure was repeated with only minor changes in the RNA amounts used in cDNA synthesis. PCR primers and cycling conditions are available upon request.

Spontaneous mutation rate and mutation spectra: Fluctuation analysis was used to determine forward mutation rates at the *CAN1* (arginine permease) locus. Cells were grown overnight in SC-Leu medium (28), serially diluted, plated on SC-complete medium (28) and incubated for a week or until the colonies reached 2-4 mm in diameter. Nine colonies from each strain were excised from the agar plates, suspended in sterile H_2O and dispersed by vortexing and sonication. Aliquots were removed to count the total number of cells and the remainder was plated on SC-Leu-Arg medium containing canavanine sulfate (Sigma, St.Louis, MO; 60 mg/ml) to select for canavanine-resistant (Can^r) cells. After 2-4 days, the number of Can^r colonies was counted and the mutation rate evaluated by using the method of the median of Lea and Coulson (30). Mutations in independent Can^r colonies were verified by PCR amplification of ~1.8 kb of *CAN1* genomic DNA using high-fidelity Ultra Pfu DNA polymerase (Stratagene, CA), followed by purification and direct sequencing of the amplified DNA. Sequences of primers used for PCR and DNA sequencing are available upon request.

Flowcytometry analysis: Fresh saturated overnight cultures were diluted to OD A_{600}~ 0.3 – 0.4, cultured at 30°C for 1 hour and synchronized by addition of 10 μg/ml of alpha mating factor; after 2.5 hrs, cells were microscopically examined for synchrony, washed twice in sterile distilled water and dispersed in pre warmed YPD. 1ml of cells were removed every 30 minutes for 300 minutes, cells were spun down and fixed in 100% ethanol. Fixed cells were washed once in 10mM Tris.HCl (pH 7.5), 10mM EDTA suspended in 0.1ml of the 10mM Tris.HCl (pH 7.5), 10mM EDTA, 0.1mg/ml RNAseA and incubated overnight at 37°C. Cells were digested with Proteinase K at a final concentration of 0.1mg/ml by incubation at 55°C for 50 minutes. Thereafter the cells were pelleted, washed once in 1X PBS, 1mM EDTA, suspended in 0.1ml of IX PBS, 1mM EDTA, 100 μg/ml Propidium Iodide. Stained cells were diluted ten times in 1X PBS, 1mM EDTA, sonicated and sorted on a Becton-Dickson Flow cytometer.

RESULTS

Eight replacements for S.cerevisiae Pol δ Leu612 yielded viable mutants: To assess the function of L612 in motif A of *S.cerevisiae* Pol δ, we used site-directed mutagenesis to create all 19 amino acid replacements. Sequence and structural conservation of motif A residues in family A and family B DNA polymerases of particular interest for this work is illustrated in Figs. 1A,B. A model of the active site of RB69 DNA polymerase, a family B member, that shows Leu415, the residue homologous to Leu612 in yeast Pol δ, is illustrated in Fig. 1C.

Of the 19 replacements for Leu612 in yeast Pol δ, we found that eight yielded viable haploid mutant strains: Ile, Val, Thr, Phe, Met, Lys, Asn and Gly. The mutant strains formed colonies at

25°C, 30°C and 37°C on both rich (YPD) and minimal (SC-Leu) media, however, with exception of L612G and L612N, colony formation and mid-log phase growth in rich and minimal media was slower when compared to wild-type and other mutant strains. All other strains exhibited a doubling time at mid-log phase similar to that of wild-type cells in YPD medium at 30°C (data not shown).

Leu612-mutants displayed differential hypersensitivity to hydroxyurea and MMS: The essentiality of Pol δ for DNA replication implies that substitutions for Leu612 might confer hypersensitivity to genotoxic agents. We therefore grew the mutants on YPD containing hydroxyurea (HU), an inhibitor of ribonucleotide reductase that diminishes dNTP pools and thereby causes replication forks to stall (31). For reference, we included the exonuclease-minus, proofreading-deficient mutant *pol3-01* (D321A, E323A) (29,32). As shown in Fig. 2, most of the Leu612 mutants exhibited reduced growth relative to that of the wild-type strain on YPD containing 50 mM HU. The variation in sensitivity was wide, with L612M being minimally affected, if at all, and L612T, L612G and L612N being severely inhibited. The relative sensitivity was as follows: L612, *pol3-01*, L612M < L612I, L612V, L612F < L612K, L612G, L612T, L612N. The greater inhibition of L612I relative to L612M was clearly evident at 75 mM HU, where L612I was inviable and both L612M and *pol3-01* grew weakly (data not shown). We conclude that the majority of the viable Leu612 mutants are hypersensitive to HU, and infer that Leu612 in wild-type Pol δ supports the ability to carry out DNA synthetic processes in the presence of reduced dNTP concentrations.

To assess the effects of replacement of Leu612 on sensitivity to alkylation, we exposed the mutants to the methylating agent methylmethanesulfonate (MMS). MMS introduces diverse methyl adducts in DNA and also causes replication forks to stall (33,34). Most of the eight Leu612 mutants showed reduced viability relative to the wild-type strain when grown on YPD containing 0.025% MMS (Fig. 2). The relative hypersensitivity of the mutants was similar to that observed for HU: L612, L612M, L612I, L612V < L612F, *pol3-01* < L612K < L612G, L612T, L612N. As in the case of HU, MMS hypersensitivity varied greatly, from slight if any (L612M, L612I, L612V) to severe (L612G, L612T, L612N). The reduced MMS resistance in many of the mutants may be indicative of a deficit in one or more of the processes in which *S. cerevisiae* Pol δ participates, e.g., replication, base excision repair of methylation damage and/or recombination (4,35,36).

In contrast to the results for MMS, the Leu612 mutants showed wild-type growth following UV irradiation at doses up to 100 J/m^2, with the exception of L612N (Fig. 2). Other Pol δ mutants as well do not display hypersensitivity to UV, a finding that has been ascribed to the function of other DNA polymerases, such as Pol ε or Pol η, in repair or tolerance of UV damage (35,37,38). However, the exceptional L612N mutant may be so severely impaired that redundant functions cannot fully compensate, thus unmasking a contribution of Pol δ to UV survival.

Leu612 mutant strains exhibited varying cell cycle defects and morphologic anomalies: Based on the role of Pol δ in replication, and the HU and MMS hypersensitivity described above, we looked for evidence of anomalous cell cycle progression in the Leu612 mutants. As shown in the fluorescence-activated cell sorting (FACS) analyses in Fig. 3, substitutions at Leu612 produced cell cycle defects of differing kinds and degree. Also, as summarized in Fig. 4A, mid-log cultures of some mutant strains contained cells with aberrant morphology. Representative morphologic anomalies in the mutant cultures, together with representative wild-type cells, ascertained by phase contrast microscopy and nuclear staining of at least 600 cells for each strain, are depicted in Fig. 4B. We describe the less affected mutants first and proceed to the most anomalous**.** The L612I, L612V, L612G and *pol3-01* mutants appeared to initiate DNA synthesis somewhat more slowly than the wild-type strain after release from α-factor arrest, as judged by an excess of cells with 1N DNA content at 30 min (Fig. 3). A similar delay has been observed previously for another *pol3-01* strain (39). In addition, the L612V mutant accumulated a disproportionately large fraction of cells with DNA content intermediate between 1N and 2N at 30 and 90 min, suggestive of prolonged S-phase. The L612T strain also showed this latter pattern. The L612M strain exhibited minimal deviation

from wild-type profiles, apart from a possible excess of cells with a DNA content intermediate between 1N and 2N at 30 min suggestive of slow S-phase progression. The L612K strain also displayed minimal deviation in FACS analysis, though the unsynchronized culture contained an elevated fraction of cells with 2N DNA content, and an apparently elevated proportion of cells with 2N DNA content was not synchronized in G1 by α-factor.

The L612G mutant was conspicuously anomalous. We observed an excess of cells with 1N DNA content, as well as a DNA content intermediate between 1N and 2N, through the initial 90 min after release from arrest. We infer that there is a delay in the onset of DNA synthesis in the L612G mutant, and slow traverse of the first S-phase following arrest. By 120 min after release, the profile in the L612G mutant resembled that in the wild-type strain at 90 min, most of the cells in both cultures having reached 2N DNA content. After 120 min, progression in the L612G mutant paralleled that seen in the wild-type strain after 90 min. Morphologic analysis of a mid-logarithmic phase culture (Fig. 4) showed a high proportion of aberrant cells, including an *ca*. 4-fold excess of large-budded dumbbell shaped cells with divided or undivided nuclei at or near the bud neck, suggestive of G2/M arrest.

The L612N mutant showed the most severe cell cycle defects. An unsynchronized culture, as well as cultures examined at ≥ 90 min after release from arrest, accumulated a large population of cells with 2N DNA content, suggestive of G2/M arrest (compare 2N peak at 90 min with 210 min in Fig. 3). Consistent with this inference, an 8-fold excess of cells in a mid-log phase culture (40% vs. 5% for wild-type) were dumbbell-shaped with undivided nuclei at or near the bud neck (Fig. 4). Additionally, the 30 min FACS profile was suggestive of prolonged S-phase (Fig. 3).

The apparent prolongation of S-phase and/or presence of a large fraction of cells with G2/M-arrest phenotype in some of the mutants is suggestive of activation of DNA damage-induced checkpoint arrest. To support this interpretation, we confirmed that the Leu612 mutants are proficient in checkpoint activation. To establish this proficiency, we used a sensitive checkpoint activation reporter in which the promoter of the damage-inducible *RNR3* gene is fused to the *E. coli lacZ* gene encoding β-galactosidase (40). As shown in Fig.5, the mutants expressed β-galactosidase when challenged with MMS, at essentially the same level as the wild-type strain.

Substitutions for Leu612 generated a mutator phenotype: Replacement of residues homologous to Leu612 in motif A in DNA polymerases from family A, family B and family Y can alter fidelity (12,14,15,20-22,41,42). Depending upon the polymerase and allele, either an increase or decrease in mutation rate, and/or altered mutation frequency *in vitro* and/or *in vivo* have been observed. To ascertain whether replacement of Leu612 in our yeast Pol δ mutants generates mutator and/or anti-mutator phenotypes, we measured forward mutation rates at the *CAN1* (arginine permease) locus in the eight viable strains. As summarized in Table 1, we observed a continuum of mutation rates from near wild-type (L612I, L612V, L612T) to 37-fold elevated (L612N). The largest elevations were obtained for L612K (13-fold), L612G (17-fold) and L612N (37-fold), the increase for L612N being similar to that seen for the *pol3-01* mutant lacking exonucleolytic proofreading (29-fold) (29,32,43). The increase for L612M (7-fold) is in accord with the 3.5-fold elevation recently reported (44). Interestingly, the increase in mutation rate was not strictly correlated with other phenotypic deficiencies. For example, the L612M mutant exhibited an increased mutation rate together with slight, if any, sensitivity to HU and MMS. Conversely, L612T mutant showed little if any elevation of mutation rate together with marked hypersensitivity to HU and MMS. To ensure that the Leu612 substitution strains were not exhibiting mutator phenotype because of altered expression of Pol δ, we quantitated the mRNA expression levels of Pol δ in all our strains and normalized to wild-type strain. The Pol δ mRNA expression levels were determined by quantitative RT-PCR using purified total RNA obtained from each of the strains during exponential growth. The fold change in the Pol δ RNA expression levels in the strains that display most profound phenotypic defects**,** L612K (13-fold), L612G (17-fold) and L612N (37-fold), was increased 2.5, 1.5, and 2.8–fold, respectively. In contrast, the reference exonuclease deficient strain, *pol3-01,* was reduced 1.7-fold compared to that of the wild-type.

Furthermore, the expression level in strains that did not significantly affect mutation rates, L612I, L612V, L612F and L612M, were +1.1, -3.5, -1.3 and -1.6-fold compared to that of the wild-type, respectively. Our analysis suggests that each different substitution for Leu612 elicits unique phenotypic defects and these defects do not correlate with small changes in the Pol δ mRNA expression levels or changes in mutation rates.

To examine the nature of the mutations arising in the Leu612 variants, we sequenced the 1.8 Kb *CAN1* gene in independent canavanine-resistant (Can^r) clones. As summarized in Table 2, and consistent with previous reports (37,39,45), the most frequent mutations in the wild-type strain were single-base substitutions, with transitions outnumbering transversions. The remaining mutations were insertions or deletions. A notable feature of the wild-type spectrum was the presence of mononucleotide runs of at least three A's or T's immediately 5' or 3' of the mutation in 52% (12/23) of the Can^r clones. An apparent propensity of wild-type strains for mutations at mononucleotide runs has been observed by others (37,39,45). The mutation spectra observed for the five L612 mutant strains with the highest mutation rates did not differ substantially from the wild-type spectrum, after analysis by Fisher's exact test, base substitutions representing the majority of sequence changes. The L612K spectrum, however, is statistically distinct (Fisher's exact test, p=0.01) from rest of the mutation spectra in including more transversions than transitions; in fact, 28% of all mutations (5/18) were T->A transversions (46). The L612K spectrum also contained the largest proportion of insertions/deletions.

DISCUSSION

In this work, we used site-specific mutagenesis and plasmid shuffling to create all 19 replacements for the highly conserved Leu612 in motif A of *S.cerevisiae* Pol δ (Fig. 1). Our rationale was based on the essential roles of Pol δ in DNA synthetic processes in eukaryotic cells, and on the importance of residues homologous to Leu612 for replication fidelity of other DNA polymerases. Eight of the 19 replacements for Leu612 supported growth, including the conservative substitutions Ile, Val, and Met, as well as the non-polar aromatic Phe. These hydrophobic residues occur naturally at the homologous position in other DNA polymerases (e.g., Fig. 1) and/or are tolerated as single substitutions in *E. coli* pol I, *Taq* pol I and/or yeast Pol α (12,14,15,20,41). The non-conservative substitutions Thr and Lys, and to a lesser extent Asn, have also been found among single replacements tolerated in pol I, while Gly has not been observed (12,14,15,20,41).

Allele-dependence of phenotype among Leu612 mutants: We examined the sensitivity of the viable mutant strains to genotoxic substances, cell cycle progression and cellular morphology, and forward mutation rate and spectra at the *CAN1* locus. Our data suggest that none of the viable mutant alleles is phenotypically silent, highlighting the importance of Leu612 for Pol δ function. Given their location at the polymerase active site (Fig. 1), the mutant amino acids may affect catalytic efficiency, base-selection fidelity, processivity and other crucial properties of the mutant polymerases. We observed a wide range in the severity of phenotypic defects, the more conservative replacements being less deleterious overall. However, there was not a strict association of specific defects among the individual mutants; this allele-dependent dissection of phenotypic deficits suggests that the mechanism(s) underlying any particular defect may differ among the mutants. We observed small fluctuations in the total mRNA levels and found no direct correlation between changes of mRNA expression and phenotypic defects among the strains. For example, the strains L612K, L612G and L612N that displayed elevated mutation rates and other phenotypic defects expressed 2 to 3-fold higher mRNA level compared to the wild-type, while the reference strain *pol3-01* which also exhibited high mutation rates displayed 2-fold lower mRNA expression level compared to the wild-type. A similar variation was observed in strains that exhibited only minimal alterations in mutation rates.

Each viable replacement for Leu612 appeared to yield a unique combination of functional deficits. The Ile, Val and Thr substitutions had little, if any, effect on mutation rate (Table I). Ile and Val were relatively innocuous overall, although both mutants showed a delay entering S-phase after release from α-

factor arrest (Fig. 3), and a particularly large fraction of L612I cells had aberrant morphology, for reasons that are not apparent (Fig. 4). In contrast, Thr conferred marked hypersensitivity to HU and MMS (Fig. 2), together with slow S-phase traverse in the first and second cycles after α factor arrest, possibly indicative of a defect in replication and/or repair of methylation damage. The Phe substitution conferred intermediate levels of deficiency overall, including a 4-fold elevation of mutation rate (Table I) and we observed predominantly base substitution errors.

The L612M replacement is of particular interest, conferring a 7-fold elevation of mutation rate (Table 1), with minimal effect on other properties examined. Apparently, the modestly error-prone L612M polymerase supports near-normal replication. This is the case even when cells are grown in the presence of HU, which requires DNA synthesis at low dNTP concentrations, or MMS, which requires concurrent Pol δ-mediated replication and base excision repair (35). Based on the relative replication proficiency, and the predominance of base substitutions in the mutation spectrum (86%; Table 2)**,** we hypothesized that the L612M mutator phenotype may reflect mainly errors made by the polymerase, rather than secondary mutagenic processes induced by defective replication. The recent work of Li et al. which was published as we completed this manuscript, sheds light on the function of the L612M polymerase (44). These authors also observed a mutator phenotype; the rate of forward mutation at *CAN1* was elevated 3.5-fold, consistent with our results. Li et al. further ascertained that mutation rates were increased in the absence of core mismatch repair proteins. The dependence of mutation rate on mismatch repair, which corrects errors that escape proofreading, suggests that the L612M mutator phenotype may in fact reflect errors made by the mutant polymerase. The L612M mutant also exhibited evidence of compromised replication, namely inviability in the absence of the *RAD27* flap endonuclease that processes Okazaki fragments, and hypersensitivity to phosphonoacetic acid, a replication inhibitor that may act as a pyrophosphate analog. Therefore, it is also possible that replication defects in the L612M mutant may induce secondary mutagenic processes that contribute to the observed mutator phenotype.

The L612 Lys, Gly and Asn replacements produced the most defective mutants overall, conferring the highest mutation rates (Table 1) together with markedly reduced growth in the presence of HU and MMS (Fig. 2). Growth of the L612N mutant was impaired even in the absence of exogenous agents (e.g., Fig. 2 and data not shown). Each of the three mutants showed anomalies in cell cycle distribution and/or morphology that are indicative of slow S-phase progression and/or arrest at G2/M-phase (Figs. 3&4). For example, asynchronous cultures of the L612K contained an excess of cells with 2N DNA content, indicative of G2/M arrest. The L612G mutant was delayed entering S-phase following release from α-factor arrest, was slow to traverse S-phase in the first cycle, and accumulated an increased proportion of large-budded, dumbbell-shaped cells that are characteristic of G2/M arrest. The L612N mutant exhibited slow S-phase and multiple, pronounced defects predominantly indicative of G2/M arrest, including an 8-fold excess of large-budded, dumbbell-shaped cells. Detection of G2/M arrested cells (Fig. 4) presumably reflects activation of a DNA damage-induced checkpoint pathways(s) triggered by endogenous DNA damage (47,48). This damage could be polymerase errors *per se*, e.g., mispaired primer termini that are not efficiently proofread and lead to frequent replication fork stalling (49). The inviability of the L612K, L612G and L612N mutants in combination with the exonuclease-minus *pol3-01* allele (data not shown) supports this interpretation. Alternatively, or in addition, the damage could be defects in newly synthesized DNA arising from reduced catalytic efficiency or altered processivity, perhaps resulting in uncoupling of lagging strand from leading strand synthesis. Whatever the nature of the damage, the poor viability in HU and MMS, and accumulation of cells with G2/M checkpoint-arrested morphology suggests perturbations at replication forks.

In budding yeast, replication forks play a critical role as both activators and primary effectors of an S-phase checkpoint pathway(s), and the activated checkpoint pathway(s) in turn leads to stabilization of stalled forks by retarding new DNA synthesis and arresting cells at G2/M

phase (33,50,51). Finally, the mutation spectra we observed for the Lys, Gly and Asn replacements further highlights the allele-dependence of phenotypes conferred by L612 substitutions. While all three spectra were dominated by base substitution errors, the L612K spectrum contained a notably high proportion of transversions and the largest fraction of deletion events observed. Interestingly, we have observed that PCR-generated mutant libraries created utilizing the *Taq* pol I mutant I614K (homologous to the yeast L612K mutant) contained ~20% of clones with deletion events while wild-type *Taq* pol I produced no deletion events (data not shown). Therefore the non conservative substitutions at L612 position in Pol δ confers strong cell cycle phenotypes during S-phase progression and leads to G2/M-phase arrest.

We utilized the *pol3-01* mutant throughout this work, in order to compare the effects of proofeading exonuclease deficiency with the effects of replacement at Leu612 in the polymerase active site. The mutation rate of the *pol3-01* mutant was elevated ~30-fold (Table I), and the mutation spectrum suggests that *pol3-01* cells accumulate base substitution errors, consistent with previous observations (32,39,43). Despite the increased mutation rate, the *pol3-01* mutant exhibited a near-normal phenotype in other respects. HU and UV sensitivity were like wild-type, and MMS sensitivity was moderately increased (Fig. 2). As previously observed, the *pol3-01* cells exhibited only subtle cell cycle defects, i.e., a slight delay in entry into S-phase after release from α factor arrest (39), similar to that seen for L612I, L612V, L612T, L612M, L612G and L612N cells. Further increase in abnormal cellular morphologies was not observed at mid-logarithmic phase. Taking the *pol3-01* phenotype as a reference, we conclude that an elevated mutation rate *per se* is not sufficient to account for the broad range of phenotypes observed among the Leu612 alleles. We propose that replacement of Leu612 may result in additional replication defects and concomitant DNA damage that causes perturbation at replication forks.

The mutator phenotype in Leu612 mutants: Replication fidelity is altered by replacement of residues homologous to Leu612 in several other DNA polymerases. Our laboratory has previously found that specific substitutions for the homologous Ile residue in *E. coli* pol I and *Taq* pol I, members of the A family of DNA polymerases, yield mutator mutants (12,15). For example, the I709F mutant of *E.coli* pol I increases mutation frequency *in vitro* and *in vivo* while maintaining wild-type catalytic efficiency (12). Among family B DNA polymerases, the L415M substitution in phage T4 DNA polymerase creates a mutator mutant that exhibits wild-type polymerase activity, increased processivity, and reduced exonuclease activity; available evidence indicates that the L415M polymerase cannot efficiently initiate transfer of DNA from the polymerase active site to the exonuclease active site, effectively reducing proofreading. The L415I substitution in T4 DNA polymerase generates an anti-mutator (21), whereas the L612I mutant of yeast Pol δ appears to have near wild-type fidelity (Table I). In this case, the effects of a specific replacement differ widely, indicative of interactions of the Ile substitution with other, polymerase-specific determinants of fidelity. In *S. cerevisiae* Pol α, the Phe, Met, Trp and Val substitutions for the homologous Leu868 create mutators of varying strength, and the human L865F polymerase is also a mutator (20). In the more distantly related family Y translesion DNA polymerases, replacement of the homologous Phe34 with Leu affects the accuracy of DNA synthesis as well (20). This brief survey indicates that wild-type Leu612 in yeast Pol δ shares an important function in fidelity with homologous residues over a broad evolutionary spectrum. The Pol δ mutants with differing mutagenic potential that we have created will be of particular value for ascertaining the mechanisms by which Leu612 contributes to wild-type replication and repair in a genetically facile eukaryotic model system.

Wild-type DNA polymerase fidelity is conferred by active site geometry that accommodates a complementary Watson-crick base pair, but excludes incorrect pairs (52,53). Proofreading of misincorporated nucleotides at the exonuclease active site contributes further to fidelity, and transit of the newly formed primer-terminus between the polymerase and exonuclease domains is a crucial process affecting accuracy. The increased mutation rate caused by replacement of Leu612 in yeast Pol δ could reflect

reduced discrimination against incorrect nucleotides at the polymerase active site. To assess this possibility, we modeled the amino acid substitutions into the active site of the family B RB69 DNA polymerase, in which Leu415 is homologous to yeast Pol δ Leu612 (54,55). The wild-type RB69 polymerase and the L415M, L415G and L415N mutant polymerases are illustrated in Fig. 6. Both the open conformation and a closed, ternary complex with an oligonucleotide primer-template and incoming dNTP are shown for each. In the wild-type ternary complex, the side chain of Leu415 is in close proximity to the sugar and α-phosphate of the incoming dNTP, and forms part of a hydrophobic region that includes Leu412, Tyr416 and Tyr567. With the exception of the L415G polymerase, close study of the models revealed no obvious changes in active site geometry that might account for reduced fidelity. (The caveat, of course, is that available crystal structures may not capture conformations in which the mutations would be predicted to alter nucleotide discrimination.) In the case of the L415G polymerase, absence of a side chain creates increased space and perhaps greater flexibility that might allow enhanced accommodation of incorrect nucleotides. We favor a model whereby the mutator phenotypes we observed may reflect, at least in part, inability of the Leu612 replacements to mediate proper partitioning between the polymerase and exonuclease active sites. This mechanism appears to contribute to the increased mutation rate of the T4 L415M polymerase (21).

In summary, we have created and analyzed a series of yeast Pol δ mutants by substitution of different amino acids for Leu612. Yeast expressing the mutant alleles exhibit diverse phenotypes that may differentially reflect the roles of Pol δ in various DNA synthetic processes. An analysis of DNA synthesized *in vivo* by the mutant polymerases may help to delineate the roles of Pol δ in leading and lagging strand replication, and in different DNA repair pathways. In addition, generation of mice harboring the mutant alleles should yield further information on the role of a mutator phenotype in the generation of tumors (56,57).

REFERENCES

1. Steitz, T. A. (1998) *Nature* **391**, 231-232
2. Burgers, P. M., Koonin, E. V., Bruford, E., Blanco, L., Burtis, K. C., Christman, M. F., Copeland, W. C., Friedberg, E. C., Hanaoka, F., Hinkle, D. C., Lawrence, C. W., Nakanishi, M., Ohmori, H., Prakash, L., Prakash, S., Reynaud, C. A., Sugino, A., Todo, T., Wang, Z., Weill, J. C., and Woodgate, R. (2001) *J Biol Chem* **276**, 43487-43490
3. Hubscher, U., Maga, G., and Spadari, S. (2002) *Annu Rev Biochem* **71**, 133-163
4. Bell, S. P., and Dutta, A. (2002) *Annu Rev Biochem* **71**, 333-374
5. Hashimoto, K., Shimizu, K., Nakashima, N., and Sugino, A. (2003) *Biochemistry* **42**, 14207-14213
6. Shcherbakova, P. V., Pavlov, Y. I., Chilkova, O., Rogozin, I. B., Johansson, E., and Kunkel, T. A. (2003) *J Biol Chem* **278**, 43770-43780
7. Shimizu, K., Hashimoto, K., Kirchner, J. M., Nakai, W., Nishikawa, H., Resnick, M. A., and Sugino, A. (2002) *J Biol Chem* **277**, 37422-37429
8. Prelich, G., Tan, C. K., Kostura, M., Mathews, M. B., So, A. G., Downey, K. M., and Stillman, B. (1987) *Nature* **326**, 517-520
9. Lee, S. H., Pan, Z. Q., Kwong, A. D., Burgers, P. M., and Hurwitz, J. (1991) *J Biol Chem* **266**, 22707-22717
10. Podust, V., Mikhailov, V., Georgaki, A., and Hubscher, U. (1992) *Chromosoma* **102**, S133-141
11. Schaaper, R. M. (1993) *J Biol Chem* **268**, 23762-23765
12. Shinkai, A., Patel, P. H., and Loeb, L. A. (2001) *J Biol Chem* **276**, 18836-18842
13. Suzuki, M., Avicola, A. K., Hood, L., and Loeb, L. A. (1997) *J Biol Chem* **272**, 11228-11235
14. Suzuki, M., Baskin, D., Hood, L., and Loeb, L. A. (1996) *Proc Natl Acad Sci U S A* **93**, 9670-9675

15. Patel, P. H., Kawate, H., Adman, E., Ashbach, M., and Loeb, L. A. (2001) *J Biol Chem* **276**, 5044-5051
16. Minnick, D. T., Bebenek, K., Osheroff, W. P., Turner, R. M., Jr., Astatke, M., Liu, L., Kunkel, T. A., and Joyce, C. M. (1999) *J Biol Chem* **274**, 3067-3075
17. Polesky, A. H., Steitz, T. A., Grindley, N. D., and Joyce, C. M. (1990) *J Biol Chem* **265**, 14579-14591
18. Dong, Q., Copeland, W. C., and Wang, T. S. (1993) *J Biol Chem* **268**, 24175-24182
19. Dong, Q., Copeland, W. C., and Wang, T. S. (1993) *J Biol Chem* **268**, 24163-24174
20. Niimi, A., Limsirichaikul, S., Yoshida, S., Iwai, S., Masutani, C., Hanaoka, F., Kool, E. T., Nishiyama, Y., and Suzuki, M. (2004) *Mol Cell Biol* **24**, 2734-2746
21. Reha-Krantz, L. J., and Nonay, R. L. (1994) *J Biol Chem* **269**, 5635-5643
22. Patel, P. H., and Loeb, L. A. (2000) *J Biol Chem* **275**, 40266-40272
23. Astatke, M., Ng, K., Grindley, N. D., and Joyce, C. M. (1998) *Proc Natl Acad Sci U S A* **95**, 3402-3407
24. Araki, H., Ropp, P. A., Johnson, A. L., Johnston, L. H., Morrison, A., and Sugino, A. (1992) *Embo J* **11**, 733-740
25. Patel, P. H., and Loeb, L. A. (2000) *Proc Natl Acad Sci U S A* **97**, 5095-5100
26. Joyce, C. M., and Steitz, T. A. (1995) *J Bacteriol* **177**, 6321-6329
27. Sambrook, J., and Russell, D. W. (2001) *Molecular cloning : a laboratory manual*, 3rd Ed. 3 vols., Cold Spring Harbor Laboratory Press, Cold Spring Harbor, N.Y.
28. Burke, D., Dawson, D., Stearns, T., and Cold Spring Harbor Laboratory. (2000) *Methods in yeast genetics : a Cold Spring Harbor Laboratory course manual*, 2000 Ed., Cold Spring Harbor Laboratory Press, Plainview, N.Y.
29. Simon, M., Giot, L., and Faye, G. (1991) *Embo J* **10**, 2165-2170
30. Lea, D. E., and Coulson, C.A. (1948) *Genetics* **49**, 248-264
31. Rosenkranz, H. S., and Levy, J. A. (1965) *Biochim Biophys Acta* **95**, 181-183
32. Morrison, A., Johnson, A. L., Johnston, L. H., and Sugino, A. (1993) *Embo J* **12**, 1467-1473
33. Tercero, J. A., and Duffle, J. F. (2001) *Nature* **412**, 553-557
34. Singer, B., and Grunberger, D. (1983) *Molecular biology of mutagens and carcinogens*, Plenum Press, New York
35. Blank, A., Kim, B., and Loeb, L. A. (1994) *Proc Natl Acad Sci U S A* **91**, 9047-9051
36. Holmes, A. M., and Haber, J. E. (1999) *Cell* **96**, 415-424
37. Kooks, R. J., Stefano Vic, L., Demas, J., and Petes, T. D. (2000) *Mol Cell Biol* **20**, 7490-7504
38. Pavlov, Y. I., Shcherbakova, P. V., and Kunkel, T. A. (2001) *Genetics* **159**, 47-64
39. Datta, A., Schmeits, J. L., Amin, N. S., Lau, P. J., Myung, K., and Kolodner, R. D. (2000) *Mol Cell* **6**, 593-603
40. Zhou, Z., and Elledge, S. J. (1992) *Genetics* **131**, 851-866
41. Shinkai, A., and Loeb, L. A. (2001) *J Biol Chem* **276**, 46759-46764
42. Reha-Krantz, L. J. (1995) *Methods Enzymol* **262**, 323-331
43. Morrison, A., and Sugino, A. (1994) *Mol Gen Genet* **242**, 289-296
44. Li, L., Murphy, K. M., Kanevets, U., and Reha-Krantz, L. J. (2005) *Genetics* **170**, 569-580
45. Tran, H. T., Keen, J. D., Kricker, M., Resnick, M. A., and Gordenin, D. A. (1997) *Mol Cell Biol* **17**, 2859-2865
46. Cariello, N. F., Piegorsch, W. W., Adams, W. T., and Skopek, T. R. (1994) *Carcinogenesis* **15**, 2281-2285
47. Weinert, T. A., Kiser, G. L., and Hartwell, L. H. (1994) *Genes Dev* **8**, 652-665
48. Gardner, R., Putnam, C. W., and Weinert, T. (1999) *Embo J* **18**, 3173-3185
49. Perrino, F. W., and Loeb, L. A. (1989) *J Biol Chem* **264**, 2898-2905
50. Lopes, M., Cotta-Ramusino, C., Pellicioli, A., Liberi, G., Plevani, P., Muzi-Falconi, M., Newlon, C. S., and Foiani, M. (2001) *Nature* **412**, 557-561
51. Tercero, J. A., Longhese, M. P., and Duffle, J. F. (2003) *Mol Cell* **11**, 1323-1336

52. Kool, E. T. (2001) *Annu Rev Biophys Biomol Struct* **30**, 1-22
53. Kunkel, T. A., and Bebenek, K. (2000) *Annu Rev Biochem* **69**, 497-529
54. Wang, J., Sattar, A. K., Wang, C. C., Karam, J. D., Konigsberg, W. H., and Steitz, T. A. (1997) *Cell* **89**, 1087-1099
55. Franklin, M. C., Wang, J., and Steitz, T. A. (2001) *Cell* **105**, 657-667
56. Goldsby, R. E., Lawrence, N. A., Hays, L. E., Olmsted, E. A., Chen, X., Singh, M., and Preston, B. D. (2001) *Nat Med* **7**, 638-639
57. Goldsby, R. E., Hays, L. E., Chen, X., Olmsted, E. A., Slayton, W. B., Spangrude, G. J., and Preston, B. D. (2002) *Proc Natl Acad Sci U S A* **99**, 15560-15565

FOOTNOTES

*We are grateful to Ellie Adman for molecular modeling and energy minimization calculations, for the drawings in Figs. 1C and 6, and for valuable discussions concerning structure-function relationships. We thank Mallika Singh for generating *pol3::KanMX* strains, Trisha Davis and Tess Yoder for technical help with flow cytometry, and Ann Blank for editing the manuscript. This work was supported by NIH grants R01 CA102029 to LAL, R01 ES 09927 and R01 CA98243 to BDP, and P01 AG01751.

[1]The abbreviations used are: Pol δ, DNA polymerase-delta; Pol ε, DNA polymerase epsilon; RT-PCR, Reverse-transcription Polymerase chain reaction; DIC, differential interference contrast; FACS, fluroresence-activated cell sorter; PBS, phosphate buffered saline; WT, Wild-type; EDTA, Ethylene diamine tetra acetic acid; *E.coli*, *Escherichia coli*; *S.cerevisiae*, *Saccharomyces cerevisiae*.

FIGURE LEGENDS

Fig. 1. **Motif A structure in family A and family B DNA polymerases and modeled active site.** A, Amino acid sequence alignment of motif A residues. Leu612 in *S.cerevisiae* Pol δ, which was analyzed here, and its homologs, are boxed. B**,** Structural alignment of motifs A, B and C in family A and family B DNA polymerases, illustrating strict conservation**.** The Cα backbone is shown. The star highlights the conserved aliphatic residue corresponding to Leu612 in *S.cerevisiae* Pol δ. Coordinates of crystal structures were obtained from Protein Data Bank (http://www.rcsb.org) and manipulated in SwissPDB viewer v3.5 software (http://www.expasy.ch). Motifs A, B and C of the polymerase active sites were superimposed, and RMS deviations calculated using the tools available in the software. The family A polymerases shown are: the Klenow fragments of DNA polymerase I from *Escherichia coli* (1KFD, black) and *Thermus aquaticus* (KlenTaq, 3KTQ, blue); T7 (bacteriophage T7, 1T7P, green); and Bst (*Bacillus stearothermophilus,* 1XWL, brown). The family B DNA polymerases shown are: RB69 (bacteriophage RB69, 1IG9, red); Tgo (*Thermococcus gorgonarius,* 1TGO, purple); D.Tok *(Desulfurococcust tok,* 1QQC, yellow); and KOD (*Pyrococcus kodakaraensis*, 1GCX, cyan), RMS deviation ranges from 0.5Å to 1.5Å. C, Polymerase active site in a ternary complex (1IG9) of the family B RB69 DNA polymerase with an oligonucleotide primer-template and dTTP (54,55). Leu415 (the homolog of Leu612 in *S.cerevisiae* Pol δ) is shown in ball-and-stick form, and is in close proximity to the sugar and α-phosphate of the incoming dTTP. The figure is labeled as follows: **A** (motif A, green), **B** (motif B, tan), **C** (motif C, blue), **P** (primer strand, silver grey), **T** (template strand, blue grey). Dark grey balls depict divalent calcium ions.

Fig. 2. **Sensitivity of Leu612 mutants to genotoxic agents.** Overnight cultures of YGL27-derived haploid strains were dispersed by sonication and cell number was counted. Cells were serially diluted 10-fold in a 96-well microtiter plate, starting with 1 x 10^7 cells/ml, and spotted on YPD plates by using a 48-pin prong replicator. Incubation was at 30^0C for 2-3 days. Plates contained either no additions (control), 0.025% MMS or 50 mM HU; UV-irradiated plates (100 J/m^2) were incubated in the dark.

Fig. 3. **Cell cycle progression of Leu612 mutants.** Cultures of BY4741-derived haploid strains at OD_{600nm} ~1.8 to 2.6 were freshly diluted to OD_{600nm} ~0.3 to 0.4 in YPD and synchronized by addition of 10 μg/ml of alpha mating factor. After 2.5 hr, cells were examined microscopically for synchrony, pelleted, washed twice with sterile distilled water and incubated in pre-warmed YPD. Aliquots were removed at 30 minute intervals and cells were spun down and fixed in 100% ethanol. Fixed cells were processed as mentioned in materials and methods and sorted by utilizing Becton-Dickinson fluorescence-activated flow cytometer and the cell cycle profiles were analyzed using the program Flowjo (Ashland, OR).

Fig. 4. **Cellular and nuclear morphology of Leu612 mutants.** Aliquots of mid-logarithmic phase cultures of YGL27-derived haploid strains (OD_{600} ~0. 7 to 1.2) were used to examine cellular morphology by phase contrast (differential interference contrast) microscopy. For nuclear morphology, cells were fixed in 70% ethanol and stained with Vectashield mounting medium (Vector Laboratory, CA) containing 4',6'-diamidino-2-phenylindole (DAPI). Images were acquired at 63X magnification using a Qimaging Retiga EX digital camera mounted on a Nikon Eclipse E600 microscope. At least 600 cells of each mutant strain were examined in each of two independent experiments. A, The proportions of cells observed in mutant strains are indicated, ascertained by examination of no fewer than 600 cells per strain in each of two independent experiments. The average of both experiments is tabulated. Unbudded cells are in G1 phase. Budded cells are in S phase or normal G2/M phase. Abnormal cells are large budded, dumbbell shaped cells with an undivided or divided nucleus, indicative of G2/M-phase (predominant fraction) and post M-phase arrest respectively. Other cells are comprised of abnormally large budded, unequal sized mother-daughter cells, multiple-budded cells, and elongated cells. B, Differential interference microscopy (DIC) images of representative anomalous cells in mutant cultures and images of the same, DAPI-stained cells are shown.

Fig. 5. **Activation of the DNA damage-inducible checkpoint reporter RNR3.** The ability of the Leu612 mutants to activate a DNA damage-inducible checkpoint leading to G2/M arrest was determined by using the reporter plasmid pZZ13. The plasmid, containing the promoter of the damage-inducible *RNR3* gene fused to *E.coli lacZ* (RNR3-LacZ) was transformed into YGL27-derived mutant cells. Cultures of all strains were diluted to OD_{600}= 0.2 to 0.25, incubated at 30°C with and without 0.012% MMS for 5 hr. Triplicate samples of MMS-treated and untreated control cells were assayed for β-galactosidase activity by monitoring hydrolysis of *o*-nitrophenyl-β-galactopyranoside (ONPG) (40).

Fig. 6. **Molecular models of RB69 DNA polymerase mutants homologous to *S.cerevisiae* Pol δ Leu612 mutants.** Coordinates of the open and closed structures of the family B RB69 gp43 DNA polymerase were obtained from Protein Data Bank (1IH7 and 1IG9, respectively). Mutations at Leu415, the residue homologous to yeast Pol δ Leu612 (Fig. 1A,B) were modeled with tools available in the suite of programs in the Molecular Operating Environment (MOE) (see http://www.chemcomp.com). Coordinates for residues with atoms within 12 Å of the mutated residue, including the nucleotides, were energy-minimized using Engh & Huber structural parameters and standard procedures available in the MOE package. Figures were generated using MOLSCRIPT and Raster3Dv2.0.

Table I

Forward mutation rates at CAN1 in strains with an amino acid substitution at Leu612 in conserved motif A of DNA polymerase δ

Strain	Rate per cell division ($x10^{-7}$)			
	Expt 1	Expt 2	Mean (95% CI)	Fold-elevation
L612	1.5	2.4	2.0 (1-3)	1
L612I	2.0	4.7	3.4 (1-6)	2
L612V	2.7	3.3	3.0 (2-4)	2
L612T	3.6	3.7	3.7 (3-4)	2
L612F	5.6	8.4	7.0 (4-10)	4
L612M	11	18	15 (8-21)	7
L612K	19	32	26 (13-38)	13
L612G	45	20	33 (8-57)	17
L612N	46	100	73 (20-126)	37
pol3-01	50	62	56 (44-68)	29

Spontaneous mutation rates were measured by fluctuation analysis using the method of the median as described in Experimental procedures. Two independent experiments were performed. Fold-elevation indicates the average of the two experiments listed relative to the average for the wild-type L612. The *pol3-01* strain contains the exonuclease proofreading-deficient Pol δ allele D321A, E323A (32).

Table II

Mutational spectra at the CAN1 locus in DNA polymerase δ Leu612 mutant strains

Errors	L612	L612F	L612M	L612K	L612N	L612G
Total	23[*]	20	21[**]	18	27 (14)	20[***]
Base substitutions	17 (74%)	14 (70%)	18 (86%)	13 (65%)	25 (93%)	19 (95%)
Transitions						
A → G				1	1	
C → T				1	14 (1)[****]	
G → A	6	2	11		2	12
T → C	5	7	5	3		1
Total	11	9	16	5	17 (4)	13
Transversions						
A → C				1		
A → T	2				1	1
C → A	1	3	2		1	2
C → G	1			1		
G → C	1			1	1	
G → T		1				2
T → A		1		5	5	1
T → G	1					
Total	6	5	2	8	8 (8)	6
Deletions	4 (17%)	6 (30%)	1 (5%)	7 (35%)	2 (7%)	1 (5%)
Insertions	2 (9%)	0	2 (10%)	0	0 (0)	0

Mutational spectra were determined by DNA sequencing of PCR-amplified *CAN1* genomic DNA from independent Can^r clones. [*]Two Can^r wild-type clones had two independent mutations. [**]Two Can^r L612M clones had two independent mutations. [***]One Can^r L612G clone had two independent mutations. [****]14 independent Can^r clones carried an identical mutation, perhaps due to a jackpot event.

A.

		Motif A										
Taq Pol I	607	V	A	L	D	Y	S	Q	I	E	L	R	617
E.coli Pol I	702	V	S	A	D	Y	S	Q	I	E	L	R	712
RB69 Pol	408	M	S	F	D	L	T	S	L	Y	P	S	418
T4 Pol	405	M	S	F	D	L	T	S	L	Y	P	S	415
Yeast Pol α	861	L	V	M	D	F	N	S	L	Y	P	S	871
Human Pol α	857	L	L	L	D	F	N	S	L	Y	P	S	867
Yeast Pol δ	605	A	T	L	D	F	N	S	L	Y	P	S	615
Human Pol δ	600	A	T	L	D	F	S	S	L	Y	P	S	610
Yeast Pol ε	637	Y	H	V	D	V	A	S	M	Y	P	N	647
Human Pol ε	623	Y	H	L	D	V	G	A	M	Y	P	N	633
Yeast Pol ζ	972	I	V	L	D	F	Q	S	L	Y	P	S	982
Human Pol ζ	2611	L	V	L	D	F	Q	S	L	Y	P	S	2621

B.

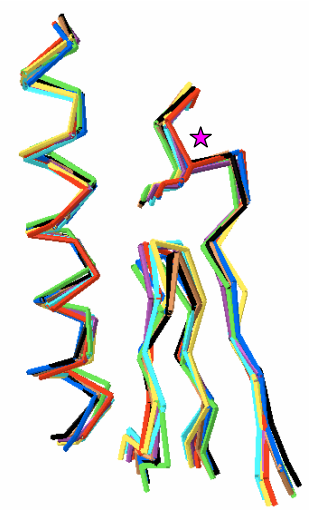

Motif B Motif C Motif A

C.

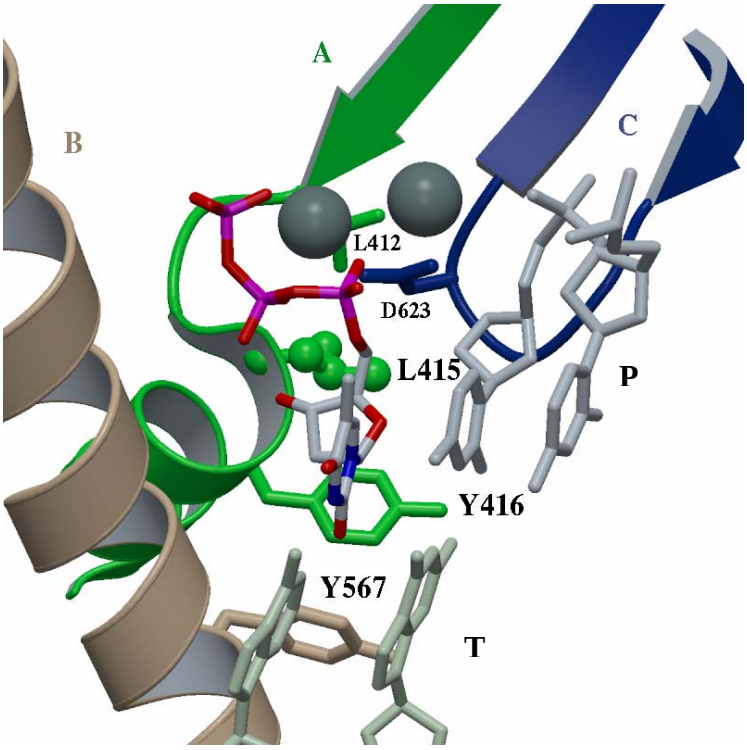

Fig. 1. Venkatesan, Hsu et al.

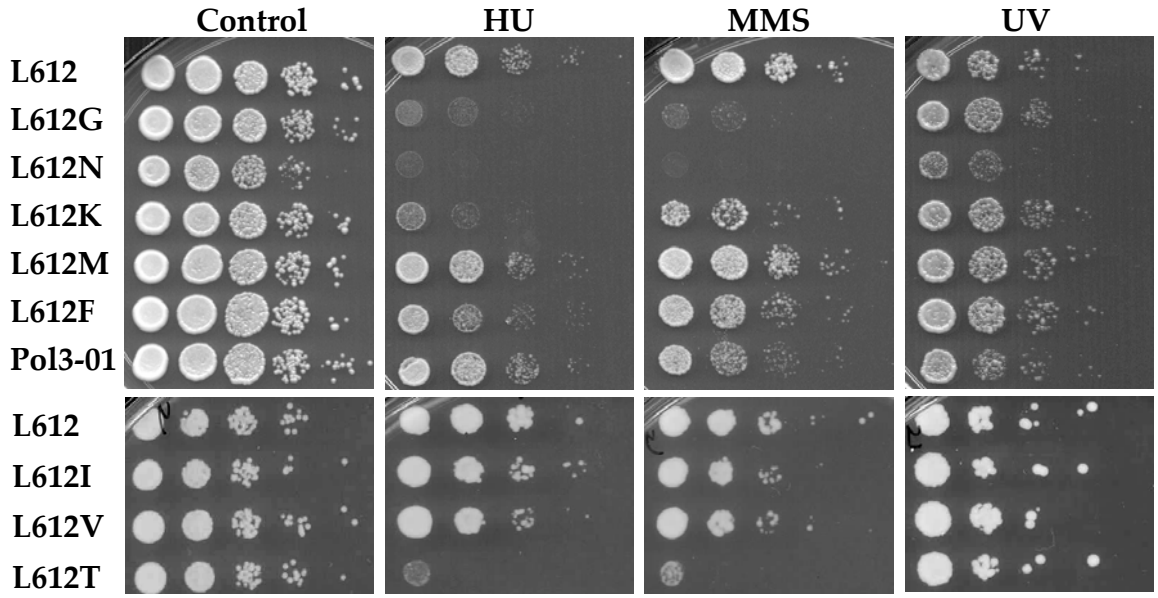

Fig. 2. Venkatesan, Hsu et al.

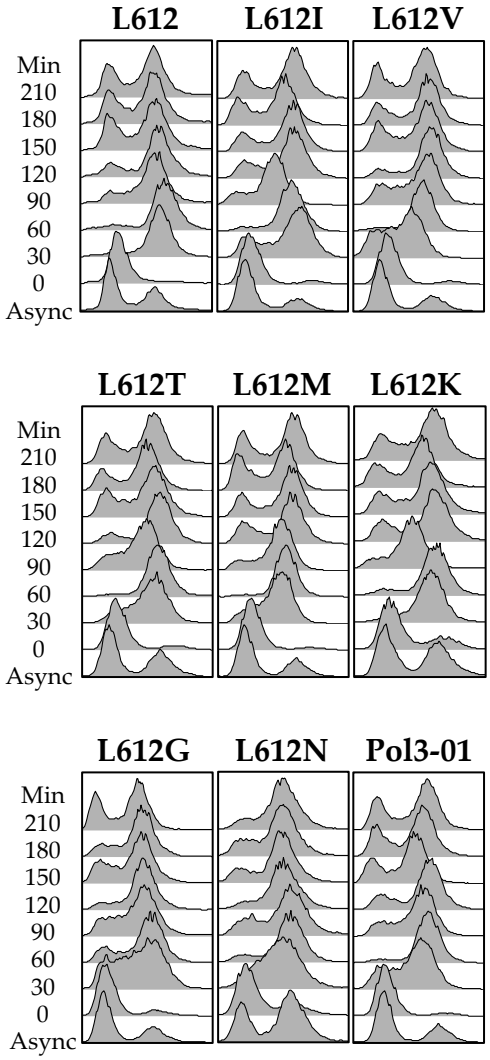

Fig. 3. Venkatesan, Hsu et al.

A.

	Unbudded (%)	Budded (%)	Abnormal (%)	Other (%)
L612	42	52	5	0
L612I	31	52	7	9
L612V	37	54	7	2
L612T	41	50	8	1
L612F	32	56	6	6
L612M	46	44	6	4
L612K	46	40	9	5
L612G	25	49	19	7
L612N	15	35	40	10
Pol3-01	50	44	5	1

B.

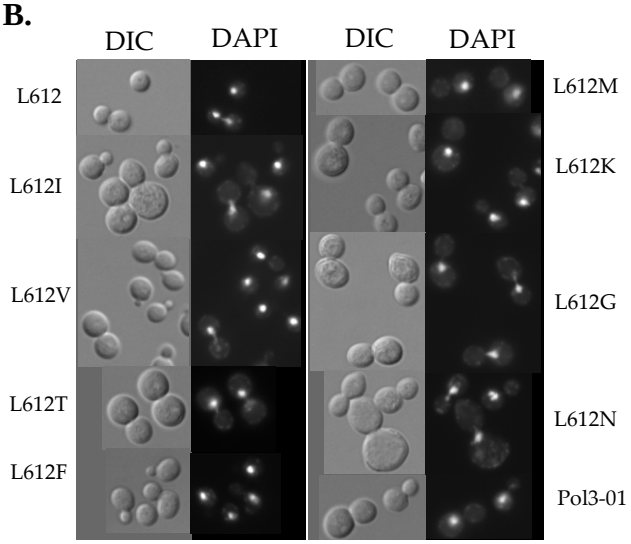

Fig. 4. Venkatesan, Hsu et al.

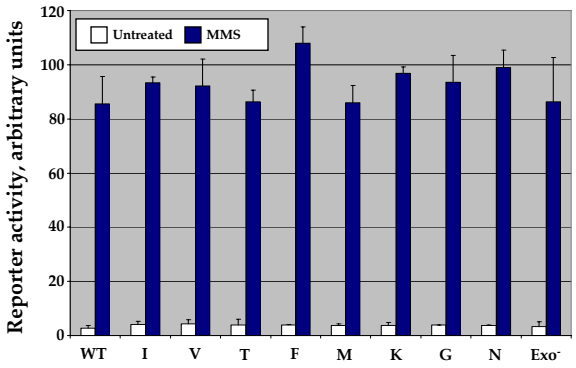

Fig. 5. Venkatesan, Hsu et al.

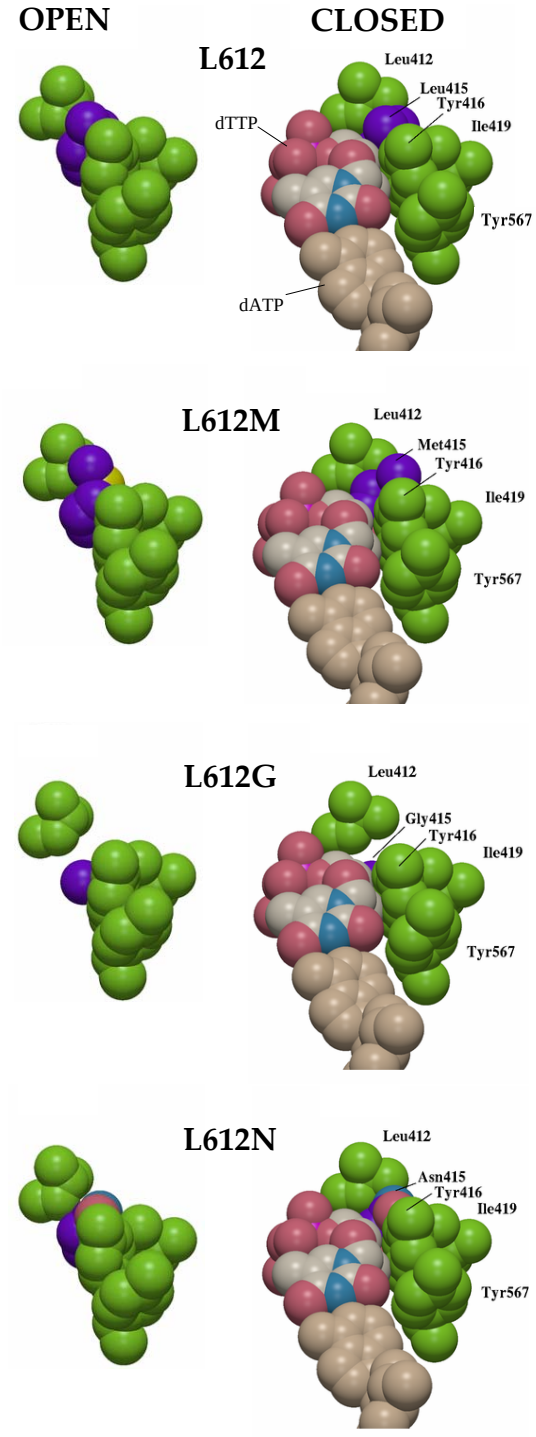

Fig. 6. Venkatesan, Hsu et al.